Journal of Solid State Chemistry 187 (2012) 323–327

Contents lists available at SciVerse ScienceDirect

Journal of Solid State Chemistry

journal homepage: www.elsevier.com/locate/jssc

Rapid Communication

Synthesis, physical properties and electronic structure of $Sr_{1-x}La_xCu_2Pn_2$ (Pn=P, As, Sb)

Mingsheng Qin [a,b], Chongyin Yang [a,b], Yaoming Wang [a,**], Zhongtian Yang [a], Ping Chen [a,b], Fuqiang Huang [a,c,*]

[a] CAS Key Laboratory of Materials for Energy Conversion, Shanghai Institute of Ceramics, Chinese Academy of Sciences, Shanghai 200050, China
[b] Graduate School of the Chinese Academy of Sciences, Beijing 100049, PR China
[c] Beijing National Laboratory for Molecular Sciences and State Key Laboratory of Rare Earth Materials Chemistry and Applications, College of Chemistry and Molecular Engineering, Peking University, Beijing 100871, China

ARTICLE INFO

Article history:
Received 21 September 2011
Received in revised form
20 December 2011
Accepted 23 December 2011
Available online 9 January 2012

Keywords:
$SrCu_2Pn_2$
Resistivity
Magnetic properties
Electronic structure

ABSTRACT

To explore new series of high-T_c superconductors, Cu-based ternary pnictides of $SrCu_2Pn_2$ (Pn=P, As, Sb) with La doping were synthesized at 1073 K from the stoichiometric reaction of the elements. The electrical and magnetic properties as well as the electronic structure were systematically investigated. Absence of superconductive transition was observed over the temperature range from room temperature down to 2 K, and these materials show *p*-type metal-like conductivity and Pauli paramagnetic behavior. The near E_F bands mainly originate from Cu 3*d* and *Pn np* states and the value of total densities of states (DOS) becomes higher as *Pn* goes from P to Sb. The results provides us with considerable information for a better understanding of the transport properties in pnictides.

1. Introduction

The discovery of the new Fe-based superconductor $LaFeAsO_{1-x}F_x$ [1,2] has motivated extensive efforts to explore new high-temperature superconductors containing a similar crystal slab of $[Fe_2As_2]^{2-}$. Recently, several new systems in Fe-based compounds such as LiFeAs [3,4], $FeSe_{1-\delta}$ [5,6], $K_xFe_{2-y}Se_2$ [7] and $AeFe_2As_2$ (Ae=Sr, Ba) have also been found to show superconductivity. As a most intensely studied group, $AeFe_2As_2$ belong to the $ThCr_2Si_2$ structure (space group no. 139, $I4/mmm$) [8,9]. Meanwhile, there are many AB_2X_2 compounds (A=alkaline earth or rare earth element; B=transition metal; X=13–15 group element) are known to crystallize in this $ThCr_2Si_2$ structure or the $CaBe_2Ge_2$ structure (space group no. 129, $P4/nmm$), which is a coloring variation of $ThCr_2Si_2$ structure. The layers in the $ThCr_2Si_2$ structure have the following feature: atoms of element *B* forms a square lattice, atoms of element *X* are located above and below the square lattice holes. In such an arrangement, the *B* atoms is at the center of the tetrahedron formed by the *X* atoms. In the $CaBe_2Ge_2$ structure *X* and *B* atoms are partially exchanged with respect to the $ThCr_2Si_2$ type [10–12]. So the $ThCr_2Si_2$ structure consists of BX_4 tetrahedra and A^{2+} layers, while the $CaBe_2Ge_2$ structure consists of BX_4 and XB_4 tetrahedra and A^{2+} layers, alternately stacked along the *c*-axis. Both $ThCr_2Si_2$-type and $CaBe_2Ge_2$-type ABX_2 compounds are excellent candidates for superconductors [13].

The superconductivity mechanism of Fe-based pnictide is unusual as a magnetic metal is incorporated [14,15], it is necessary to investigate the possibility of completely replacing Fe by nonmagnetic metal to resolve the ambiguity. The report of $LiCu_2P_2$ [16] superconductor which has a $ThCr_2Si_2$-type structure lead to explore more novel Cu-based pnictides superconductors without magnetic elements. Among the Cu-based pnictides, the $SrCu_2Pn_2$ (Pn=P, As, Sb) have both $ThCr_2Si_2$-type and $CaBe_2Ge_2$-type structure (Fig. 1) as *Pn* goes from P, As to Sb due to the decreasing Cu–Cu bonding and increasing Cu–*Pn* bonding while the *Pn* size increases [17]. It seems worth to study the superconducting properties of $SrCu_2Pn_2$ with both $ThCr_2Si_2$-type and $CaBe_2Ge_2$-type structure, even so, only the electronic structure of $AeCu_2As_2$ (Ae=Sr, Ba) was partially investigated [18], while the electrical and magnetic properties are still unknown. In this paper, the samples of $SrCu_2Pn_2$ (Pn=P, As, Sb) were prepared by high-temperature solid state reactions. The conductivity and carrier concentration of these pnictides were effectively adjusted by doping La in the Sr site. The electrical and magnetic properties

* Corresponding author at: CAS Key Laboratory of Materials for Energy Conversion, Shanghai Institute of Ceramics, Chinese Academy of Sciences, Shanghai 200050, China. Fax: +86 21 5241 3903.
** Corresponding author.
E-mail addresses: wangyaoming@mail.sic.ac.cn (Y. Wang), huangfq@mail.sic.ac.cn (F. Huang).

0022-4596/$ - see front matter © 2012 Elsevier Inc. All rights reserved.
doi:10.1016/j.jssc.2011.12.026

of $SrCu_2Pn_2$ were fully investigated. The structure analyses and the first-principles calculations were employed to further verify the experiment results.

2. Experimental

The $Sr_{1-x}La_xCu_2Pn_2$ (Pn=P, As, Sb) powders were synthesized in a stoichiometric reaction of Sr (99.999%, SinoReag), La (99.999%, SinoReag), Cu (99.999%, SinoReag), and the respective pnictide element P (99.999%, SinoReag), As (99.999%, SinoReag) and Sb (99.999%, SinoReag). Stoichiometric amounts of these raw materials were manually mixed in an Ar-filled glove box and put into an alumina crucible, the crucible was sealed in an evacuated fused silica tube, slowly heated to 1073 K at 1 K/min, held for 48 h, and then cooled in the furnace down to room temperature. The harvested powders were pressed into $\varnothing 10\,mm \times 3\,mm$ pellets under a uniaxial pressure of 12 MPa. The pellets were sealed in fused silica tubes and sintered at 973 K for 24 h.

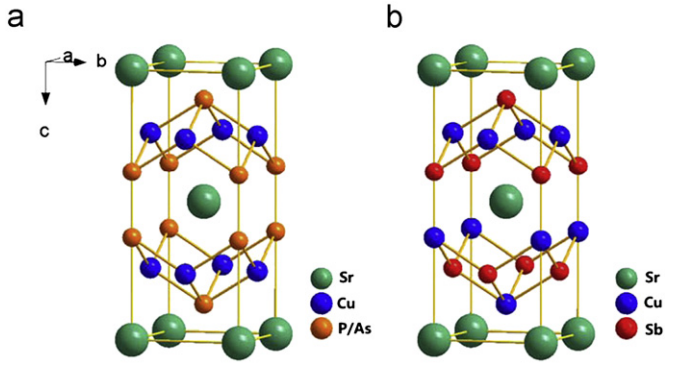

Fig. 1. Crystal structures of (a) the $ThCr_2Si_2$-type $SrCu_2Pn_2$ (Pn=P, As) and (b) the $CaBe_2Ge_2$-type $SrCu_2Sb_2$.

The X-ray diffraction (XRD) patterns of the sintered samples were recorded with a Bruker D8 FOCUS using Cu$K\alpha$ radiation (λ=1.5418 Å). The DC electrical resistivities were measured by the standard four-probe technique with silver-paint contacts from room temperature (RT) down to 2 K in a Physical Property Measurement System (PPMS; Quantum Design Company). The Hall coefficients were measured by the standard 5-wire technique with silver-paint contacts at room temperature in PPMS. Magnetic measurements were carried out using a vibrating sample magnetometer in PPMS. Temperature dependences of the magnetization were measured in a magnetic field at 10 Oe after zero-field cooling (ZFC) to the desired temperatures.

The PBE version of the generalized gradient approximation (GGA) was used to describe the exchange correlation functional, and the projector augmented wave (PAW) method was applied in the present density-functional theory (DFT) calculations [19,20]. Here, the cutoff energy of plane wave was chosen at 350 eV. For the Brillouin zone integration, $8\times8\times8$, $8\times8\times8$, $8\times8\times4$

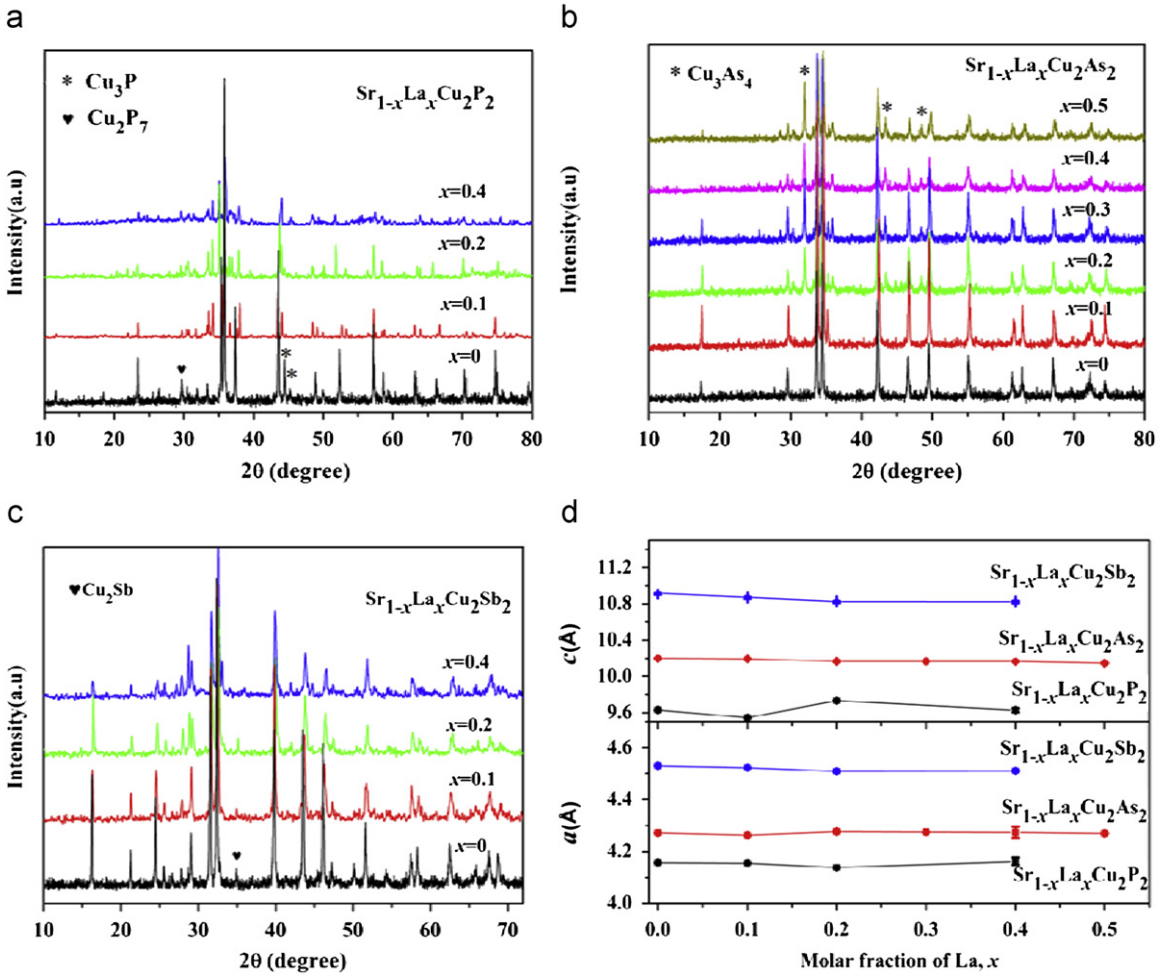

Fig. 2. The powder XRD patterns and crystal parameters of $Sr_{1-x}La_xCu_2Pn_2$ (Pn=P, As, Sb) samples. (a) $SrCu_2P_2$, (b) $SrCu_2As_2$, (c) $SrCu_2Sb_2$ and (d) lattice parameters of $Sr_{1-x}La_xCu_2Pn_2$.

Γ-centered Monkhorst–Pack grids were performed in $SrCu_2Pn_2$ (Pn=P, As, Sb), respectively.

3. Results and discussion

The X-ray diffraction patterns of synthesized $Sr_{1-x}La_xCu_2Pn_2$ are displayed in Fig. 2. The diffraction peaks of undoped samples can be indexed based on the calculation value by PowderCell for $SrCu_2P_2$ and the ICSD cards for $SrCu_2As_2$ (PDF# 85-2035) and for $SrCu_2Sb_2$ (PDF# 78-1135) [21–23]. As shown in Fig. 2, there are some Cu–Pn binary impurities in the $Sr_{1-x}La_xCu_2P_2$ and $Sr_{1-x}La_x$-Cu_2Sb_2 samples, and the as-prepared $SrCu_2As_2$ and $Sr_{0.9}La_{0.1}$-Cu_2As_2 are pure, but in the 0.2 mol La-doped sample the Cu_3As_4 impurity appeared. The lattice parameters of a and c generally decrease because the Shannon ionic radius of La^{3+} (1.03 Å) is smaller than that of Sr^{2+} (1.18 Å) [24]. The obtained samples are dark gray and chemically stable in air.

Temperature dependence of resistivities at zero magnetic field for $Sr_{1-x}La_xCu_2Pn_2$ (Pn=P, As, Sb) samples are shown in Fig. 3. No superconductivity is observed from 2 to 300 K in $Sr_{1-x}La_xCu_2Pn_2$ samples, and the resistivities displays a typical metallic behavior over the whole measured temperature range: as temperature is lowered, the electrical resistivity decreases monotonously down to 10 K, and then keeps almost constant in the temperature range 2–10 K. The resistivities of $SrCu_2Pn_2$ gradually decrease as Pn goes from P to Sb. The residual resistivities (ρ_0) and the room temperature resistivities (ρ_R) are shown in Table 1. At room temperature, the resistivity is about $7.6\times10^{-6}\,\Omega$ m for $SrCu_2P_2$, $1.2\times10^{-6}\,\Omega$ m for $SrCu_2As_2$ and $7.3\times10^{-7}\,\Omega$ m for $SrCu_2Sb_2$.

The absence of superconductivity in $Sr_{1-x}La_xCu_2Pn_2$ can be further confirmed by the magnetization data (Fig. 4a), which shows the temperature dependence of DC magnetization for the zero field cooled samples of $SrCu_2Sb_2$ and $La_{0.2}Sr_{0.8}Cu_2Sb_2$ at 10 Oe. The temperature dependence of the mass magnetization is as small as $\sim1\times10^{-4}$ emu, the well-defined Curie–Weiss

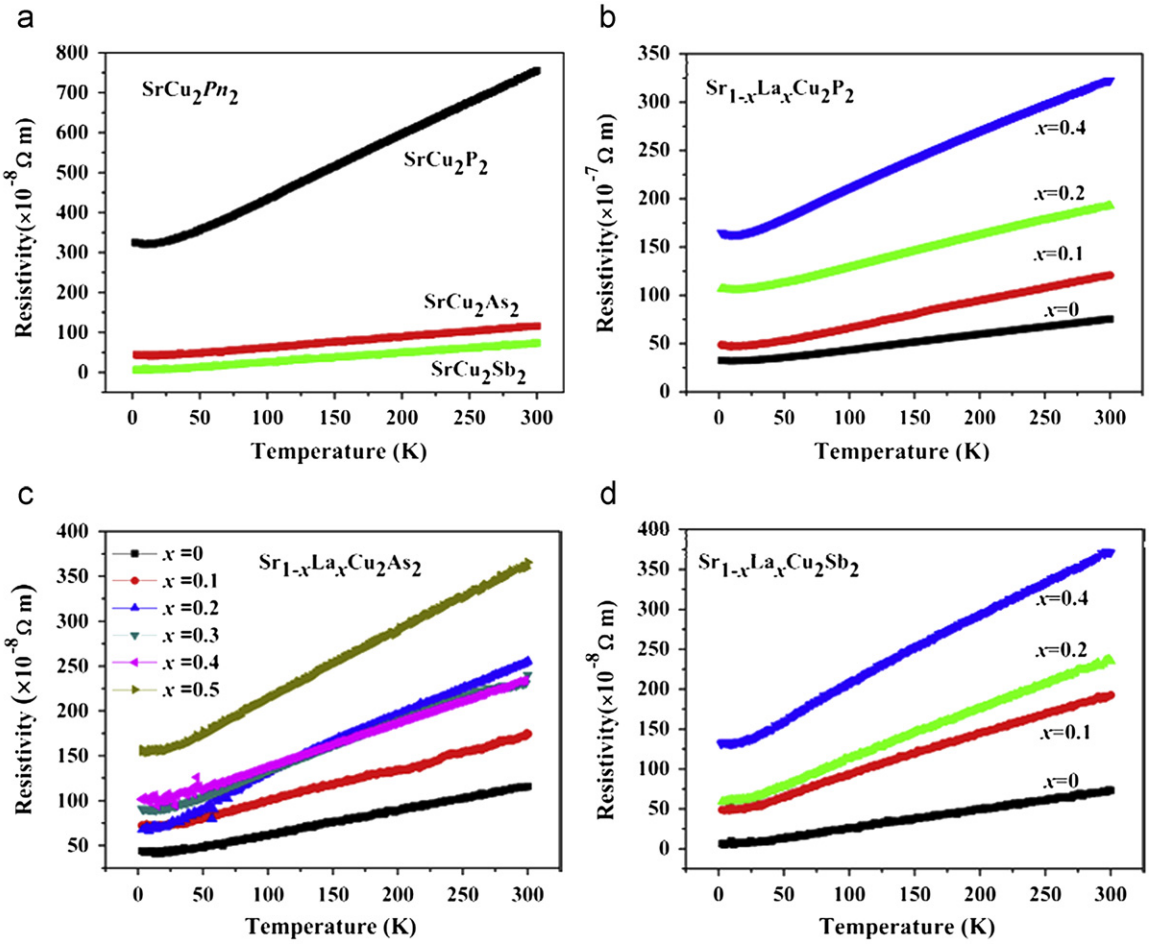

Fig. 3. Temperature dependence of the resistivity at H=0 Oe of (a) $SrCu_2Pn_2$, (b) $Sr_{1-x}La_xCu_2P_2$, (c) $Sr_{1-x}La_xCu_2As_2$ and (d) $Sr_{1-x}La_xCu_2Sb_2$.

Table 1
The lattice parameters and resistivities of $SrCu_2Pn_2$.

Sample	Space group	a (Å)	c (Å)	Cu…Cu (Å)	Cu…Pn (Å)	$r(Pn^{3-})$ (Å)	ρ_R ($\times10^{-8}\,\Omega$ m)	ρ_0 ($\times10^{-8}\,\Omega$ m)
$SrCu_2P_2$	$I4/mmm$	4.157 ± 0.001	9.633 ± 0.003	2.945	2.431	0.44[24]	755.29	323
$SrCu_2As_2$	$I4/mmm$	4.272 ± 0.002	10.199 ± 0.001	3.025	2.510	0.58[24]	116.05	42
$SrCu_2Sb_2$	$P4/nmm$	4.508 ± 0.001	10.925 ± 0.001	3.189	2.666	0.74[24]	73.21	6

ρ_0—residual resistivity, ρ_R—the resistivity at room temperature.

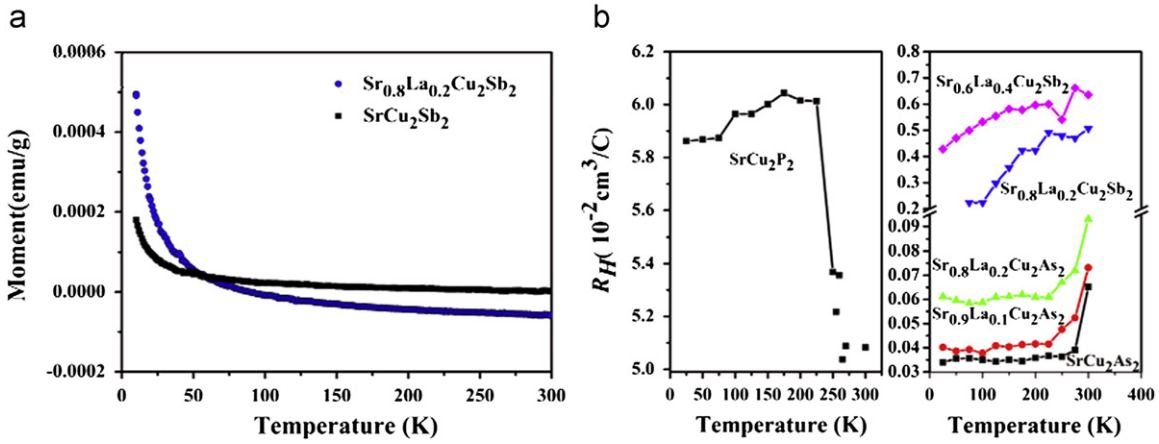

Fig. 4. (a) Temperature dependence of the mass magnetization M measured at 10 Oe after cooling to 2 K under a zero magnetic field for $Sr_{1-x}La_xCu_2Sb_2$ samples and (b) temperature dependence of the Hall coefficient R_H determined on the $Sr_{1-x}La_xCu_2Pn_2$ (Pn=P, As, Sb) samples.

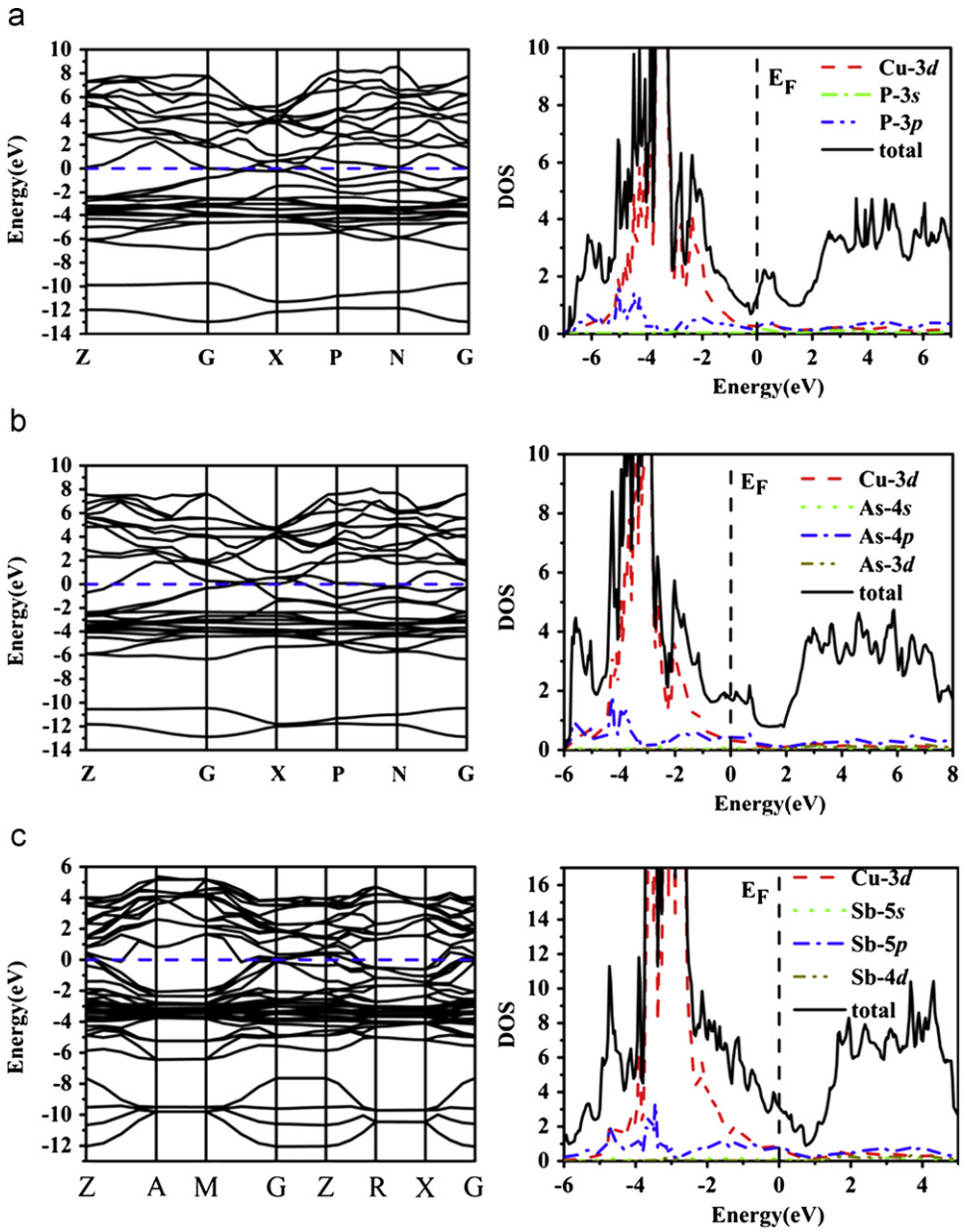

Fig. 5. The band structures and densities of states (DOS) of. (a) $SrCu_2P_2$, (b) $SrCu_2As_2$ and (c) $SrCu_2Sb_2$.

behavior and Pauli paramagnetism were observed in the whole temperature region from 2 to 300 K, and no obvious magnetic transition was observed down to 2 K. To further understand the conducting carriers in the present samples, the Hall coefficient measurements on the polycrystalline $Sr_{1-x}La_xCu_2Pn_2$ are also carried out (Fig. 4b). It is clear that the Hall coefficient R_H is positive at all temperatures below 300 K for $Sr_{1-x}La_xCu_2Pn_2$, which indicates that hole-type charge carriers dominate the conduction in the sample. Hardly any temperature-dependent variation was observed in the whole temperature region. The R_H value of $Sr_{1-x}La_xCu_2Pn_2$ is remarkably small, indicating a relatively high density of charge carriers. For example, the value of R_H is stable at around $6\times10^{-2}\,cm^3/C$ for $SrCu_2P_2$ and $3.5\times10^{-4}\,cm^3/C$ for $SrCu_2As_2$ in wide temperature, the carrier concentration is estimated to be of the order of $10^{20}\,cm^{-3}$ for $SrCu_2P_2$ and $10^{22}\,cm^{-3}$ for $SrCu_2As_2$ from the Hall coefficient by $n=1/(R_He)$.

To further confirm the electronic structure character of $SrCu_2Pn_2$, the electron band structures and total densities of states (DOS) first-principles theoretical calculations are also carried out. Unlike the former report of $AeCu_2As_2$ (Ae=Sr, Ba) electronic structure [18,25] in which the near E_F bands originate from Cu *sp* and As 4*p* states, the $SrCu_2Pn_2$ have an electronic structure similar to $LiCu_2P_2$ [26]. As shown in Fig. 5, all $SrCu_2P_2$, $SrCu_2As_2$ and $SrCu_2Sb_2$ are metallic. As *Pn* goes from P to Sb, the distorted tetrahedral [$CuPn_4$] (and [$PnCu_4$]) and the associated crystal-field splitting impart a Cu 3*d*-*Pn np* hybridization. The DOS around E_F originate mainly from this hybridization, which are responsible for the covalent Cu–*Pn* bonding. This strong hybrid behavior unlocalizes holes to provide high mobility *p*-type framework paths, which is responsible for the higher resistivity results. The value of DOS becomes higher as *Pn* goes from P to Sb because there are more electrons in the systems.

4. Conclusions

In summary, Cu-based ternary pnictide $Sr_{1-x}La_xCu_2Pn_2$ (*Pn*=P, As, Sb) were synthesized by solid-state reaction at 1073 K from the stoichiometric reaction of the elements. No superconductive transition was found for the compounds in resistivity or magnetization experiments in the temperature range from 2 K to 300 K. A metallic behavior can be seen in resistivity, and a paramagnetic behavior was observed in DC magnetization from 2 to 300 K. The Hall coefficient of the polycrystalline $Sr_{1-x}La_xCu_2Pn_2$ are positive and slight temperature-dependent variation. The value of DOS becomes higher as *Pn* goes from P to Sb, and the near E_F bands mainly originate from the hybridization of Cu 3*d* and *Pn np* states.

Acknowledgments

This work was financially supported by National 973/863 Program of China Grants 2009CB939903 & 2011AA050505; NSF of China Grants 91122034, 51125006, 50821004, 21101164, 61076062, 51102263, & 61106088; and Science and Technology Commission of Shanghai Grants 10520706700 & 10JC1415800.

References

[1] Y. Kamihara, T. Watanabe, M. Hirano, H. Hosono, J. Am. Chem. Soc. 130 (2008) 3296–3297.
[2] G.F. Chen, Z. Li, G. Zhou, D. Wu, J. Dong, W.Z. Hu, P. Zheng, Z.J. Chen, J.L. Luo, N.L. Wang, Phys. Rev. Lett. 101 (2008) 057007.
[3] J.H. Tapp, Z. Tang, B. Lv, K. Sasmal, B. Lorenz, P.C.W. Chu, A.M. Guloy, Phys. Rev. B 78 (2008) 060505.
[4] X.C. Wang, Q.Q. Liu, Y.X. Lv, W.B. Gao, L.X. Yang, R.C. Yu, F.Y. Li, C.Q. Jin, Solid State Commun. 11–12 (2008) 538.
[5] F. Ronning, T. Klimczuk, E.D. Bauer, H. Volz, J.D. Thompson, J. Phys.: Condens. Matter 20 (2008) 322201.
[6] R. Viennois, E. Giannini, D. van der Marel, R. Cerny, J. Solid State Chem. 183 (2010) 769–775.
[7] J. Guo, S. Jin, G. Wang, S. Wang, K. Zhu, T. Zhou, M. He, X. Chen, Phys. Rev. B 82 (2010) 180520.
[8] M. Rotter, M. Tegel, D. Johrendt, Phys. Rev. Lett. 101 (2008) 107006.
[9] E. Gustenau, P. Herzig, A. Neckel, J. Alloys Compd. 262–263 (1997) 516–520.
[10] P.C. Canfield, S.L. Bud'ko, Annu. Rev. Condens. Matter Phys. 1 (2010) 27.
[11] D.C. Johnston, Adv. Phys. 59 (2010) 803.
[12] C. Zheng, R. Hoffmann, J. Am. Chem. Soc. 108 (1986) 3078–3088.
[13] R.N. Shelton, H.F. Braun, E. Musik, Solid State Commun. 52 (1984) 197–799.
[14] D.J. Singh, Phys. Rev. B 78 (2008) 094511.
[15] J. Zhao, D.T. Adroja, D.X. Yao, R. Bewley, S. Li, X.F. Wang, G. Wu, X.H. Chen, J. Hu, P. Dai, Nat. Phys. 5 (2009) 555.
[16] J.T. Han, J.S. Zhou, J.G. Cheng, J.B. Goodenough, J. Am. Chem. Soc. 132 (2010) 908–909.
[17] W.K. Hofmann, W. Jeitschko, Monatsh. Chem. 116 (1985) 569.
[18] D.J. Singh, Phys. Rev. B 79 (2009) 153102.
[19] J.P. Perdew, K. Burke, M. Ernzerhof, Phys. Rev. Lett. 77 (1996) 3865–3868.
[20] P.E. Blchl, Phys. Rev. B 50 (1994) 17953.
[21] W. Kraus, G. Nolze, Federal Institute for Materials Research and Testing, Berlin, PowderCell for Windows Version 2.3, 1999.
[22] J. Duenner, A. Mewis, M. Roepke, G. Michels, Z. Anorg. Allg. Chem. 621 (1995) 1523–1530.
[23] G. Cordier, B. Eisenmann, H. Schaefer, Z. Anorg. Allg. Chem. 426 (1976) 205–214.
[24] R.D. Shannon, Acta Crystallogr. A32 (1976) 751–767.
[25] E.D. Mun, S.L. Bud'ko, N. Ni, A.N. Thaler, P.C. Canfield, Phys. Rev. B 80 (2009) 054517.
[26] I.R. Shein, A.L. Ivanovskii, Physica C 471 (2011) 226–228.